# MATERIAL DENSITY DISTRIBUTION OF A RADIAL SYMMETRIC PRODUCT FROM A SINGLE X-RAY RADIOGRAPH

A. Notea*, D. Pal*, and M. Deutsch**

*Quality Assurance and Reliability
Technion, Haifa, Israel
**Physics Department
Bar-Ilan University
Ramat-Gan, Israel

## INTRODUCTION

X-ray digital tomographic methods may be classified according to the number of projections and the angular coverage required to obtain the density distribution of the object under study. At one extremity stands computerized tomography which employs multiple projections and wide angular coverage ($\pm \pi$). At the other extremity stand reconstruction methods employing a single projection. As the number of projections decreases, the information provided for the reconstruction becomes more incomplete. The decrease in the information content may sometimes be compensated by the use of a priori knowledge about the product and thus alleviate to some extent the ill-posedness of the problem [1-4].

In this study, results of reconstruction from a single projection are presented. The solution is possible under the imposed constraint that the examined product is cylindrically symmetric in material density and elemental composition. In this method, variation of the linear attenuation coefficient for a parallel beam of x-rays across the examined product is reconstructed from the grey level distribution of a radiographic image using the inverse Abel transform.

In previous studies by the present authors, the spline-based method for reconstruction of a continuous radial density profile [5,6], and the intervals method for discontinuous profiles [7,8], were studied. Here, the application of the methods to radiographs of several test and commercial objects are demonstrated.

## PRINCIPLES

The grey level profile, $D(y)$, along a line perpendicular to the axis of symmetry in the radiographic image of a cylindrically symmetric object of outer radius, $R$, is related to the radial distribution of the linear absorption coefficient, $g(r)$, by the Abel transform:

*Review of Progress in Quantitative Nondestructive Evaluation*, Vol. 9
Edited by D.O. Thompson and D.E. Chimenti
Plenum Press, New York, 1990

$$I(y) = C - D(y) = 2 \int_y^R g(r) r (r^2 - y^2)^{-\frac{1}{2}} dy \qquad (1)$$

where C is the grey level at a point where no attenuating medium is present.

For the inversion of the Abel transform, an approach based on piece-wise cubic spline fitting [9,10] was used. At points of discontinuity of the linear attenuation distribution, the reconstructed image exhibits deviations due to the Gibbs phenomena. The effect significantly (~10%) distorts the reconstructed profile in the neighbourhood of the discontinuity [7]. To overcome such artifacts, a method [7] (denoted hereafter by DNP) based on the direct Abel transform was developed. In this method, g(r) is represented by

$$g(r) = \sum_{i=1}^{N} g_i(r) \qquad (2)$$

where N is the number of discontinuities at $R_i$ (i = 0,1,...,N), and in each interval $[R_{i-1}, R_i]$, the $g_i(r)$ is smooth and continuous and given by a k-th order polynomial

$$g_i(r) = \begin{cases} \sum_{k=0}^{K} a_{ki} r^k & R_{i-1} \leq r \leq R_i \\ 0 & r < R_{i-1};\ r > R_i \end{cases} \qquad (3)$$

Substituting g(r) in I(y), Eq.(1), and least-square fitting the resulting expression to the measured I(y) data, the sets of $\{a_{ki}\}$ and $\{R_i\}$ are obtained. The determined g(r) is free of the Gibbs effects. When it is known a priori that $g_i$ are constant within each interval, the resultant I(y) is given by a sum of ellipses:

$$I(y) = 2 \left[ \sum_{n=j}^{N-1} (a_n - a_{n+1}) (R_n^2 - y^2)^{\frac{1}{2}} + a_N (R_N^2 - y^2)^{\frac{1}{2}} \right] \qquad (4)$$

The solution here is recursive starting from the outside surface of the examined object. In the following, this method is referred to as the "onion peeling method".

The various methods are summarized in Fig. 1. Whenever a priori information on the piece-wise constancy, or otherwise, of g(r), is not available the spline-based Abel transform should be applied even for discontinuous g, to obtain estimates for the $\{a_{ki}\}$.

## RESULTS

An object made of three concentric rings of aluminum, lucite and graphite, was radiographed (130 kV, 60 mA-min, FFD 2.25 m and film D7). The densitometrically-scanned profile, I(y), is shown in Fig. 2. The digitization was performed by an automatic microdensitometer (Photomation 1700, Optronics Inc., USA) with an aperture of 200 x 200 μm.

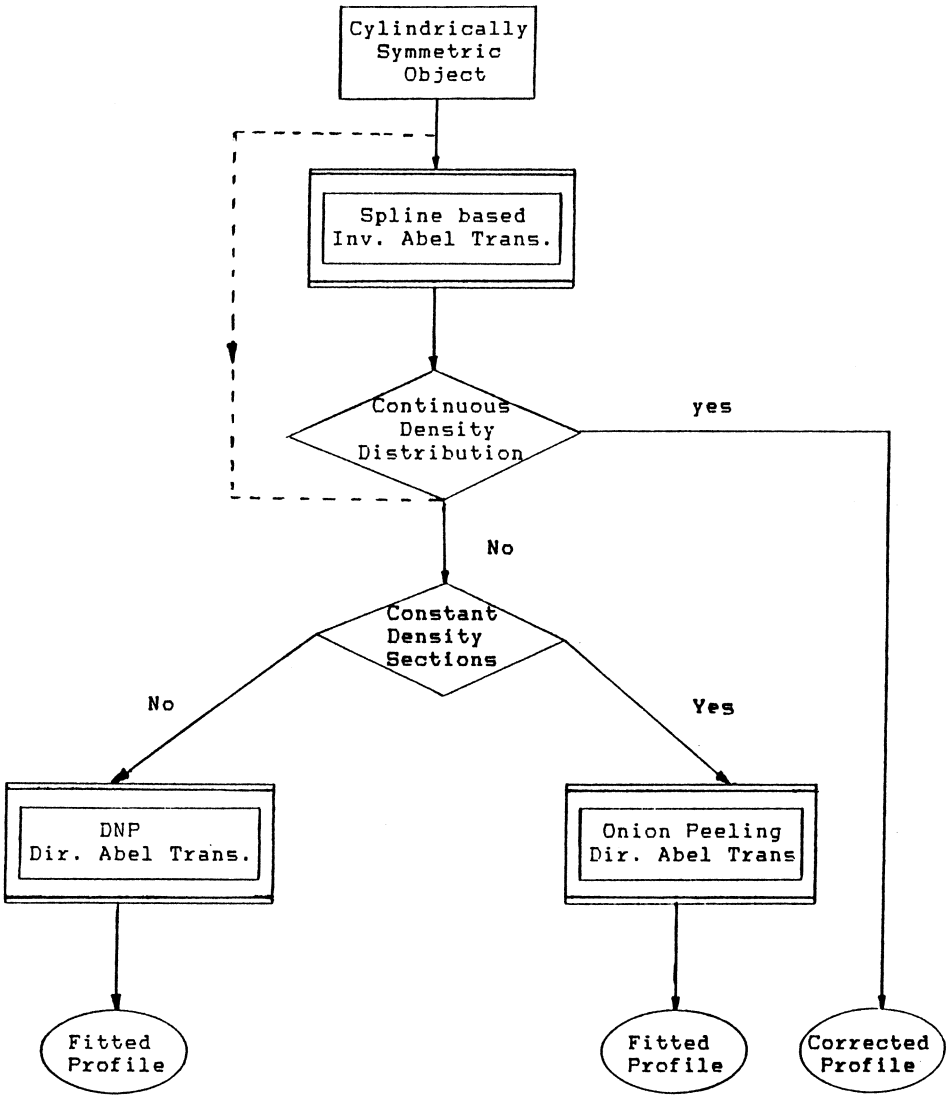


Fig. 1 Reconstruction methods based on direct and inverse Abel transform.

The profile was reconstructed using the continuous spline-based method and the results, shown in Fig. 2, indicate constant values for g(r) of the graphite and lucite rings. For the aluminum ring, the rise in g is due to the beam-hardening effect, and the strong distortion caused by the Gibbs phenomena is observed at the outer edge. The latter disappears when the DNP is used, see Fig. 2d. The ratios between the average g values in each section are similar to those of the linear attenuation coefficients of the relevant materials as found in the literature.

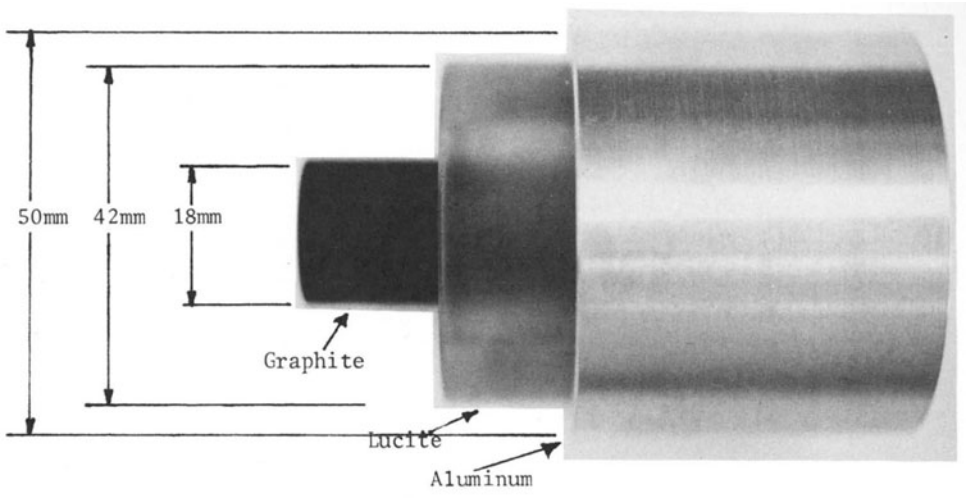


Fig. 2 (a)

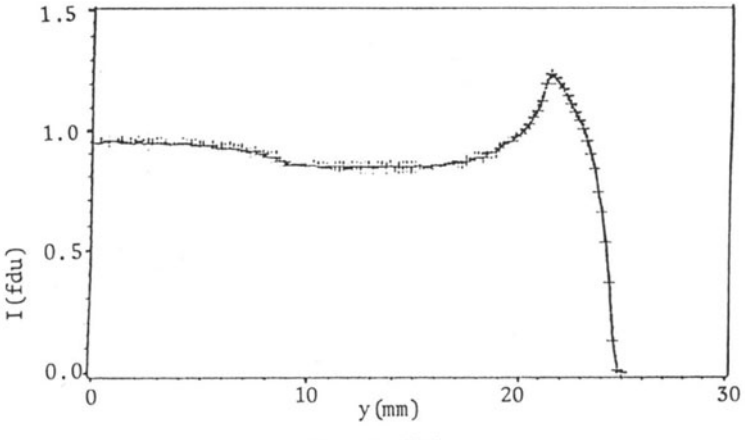


Fig. 2 (b)

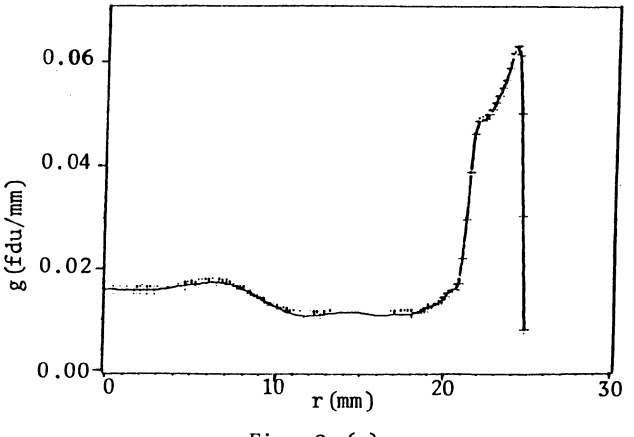


Fig. 2 (c)

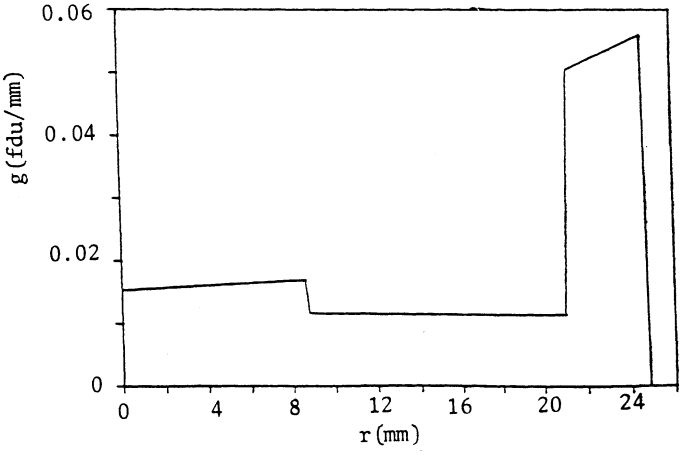


(d)

Fig. 2 Aluminum, lucite and graphite concentric cylinders (a). Profile from the radiographs averaged over 100 lines (b). Reconstructed profile by the spline-based inverse Abel transform (c). Reconstruction by the DNP method (d).

The beam-hardening effect is demonstrated for an aluminum cylinder (1.46 cm radius) radiographed with polyenergetic (X-ray source 130 kV, 15 mV-min, FFD 2.25 cm) and monoenergetic (Cs-137 radioactive source, 7 Ci, 90 min., FFD 0.87 m) beams. In the reconstructed profiles, Fig. 3, the beam hardening of the polyenergetic beam is observed in the outer layer

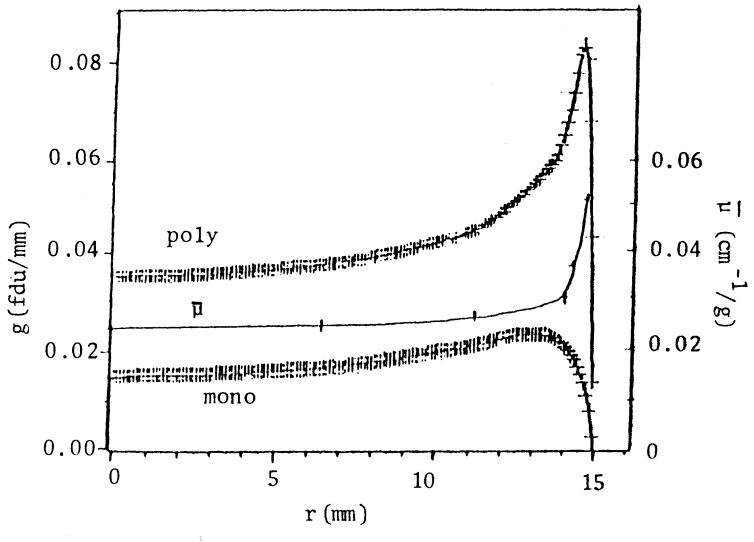


Fig. 3 Reconstructed profiles from radiographs of an Aℓ cylinder (1.46 cm radius) with 130 kV x-rays (poly) and Cs-137 gamma rays (mono). Average attenuation coefficient for 130 kV is indicated by $\bar{\mu}$.

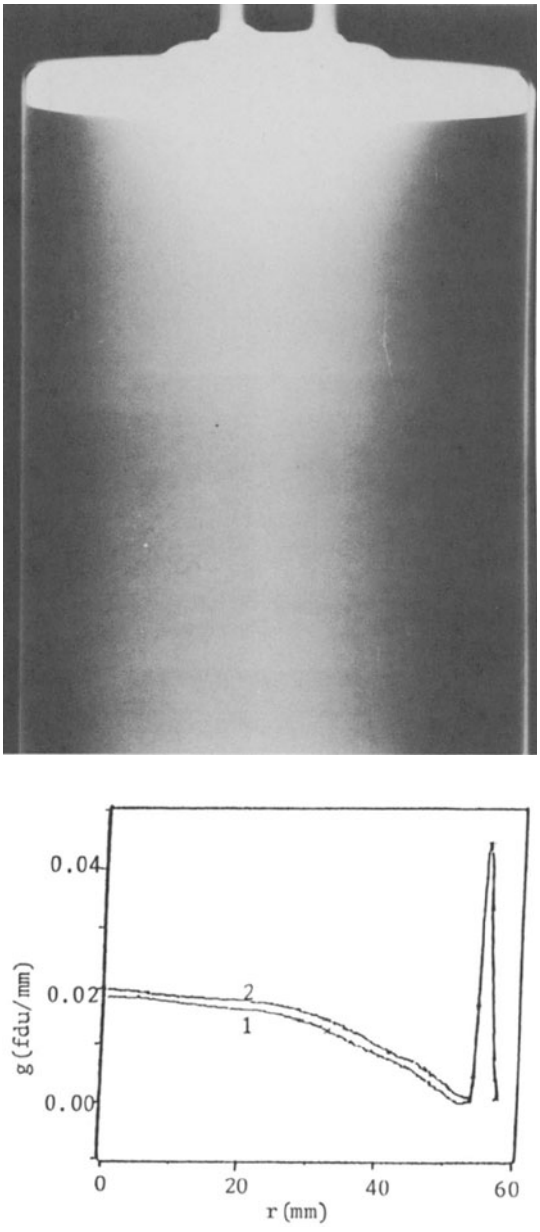


Fig. 4 Radiograph of an illumination candle (top) and reconstructed profiles (bottom).

(from about 10 mm) of the cylinder. For comparison, the behavior of the average attenuation coefficient for 140 kV radiation with W target is presented. The slow rise in the g obtained by the monoenergetic beam results from the relatively short FFD. The radiographic image of the upper part of an illumination candle (5.7 cm radius) was generated (290 kV, 25 mA-min, FFD 2.5 m, D4 F/B 0.1 mm Pb), Fig. 4, and profiles at the indicated positions were reconstructed. As is seen, g decreases towards the metallic wall which is represented by a sharp peak.

Another product examined was a propellant in a metallic case of 6 cm radius, with a cylindrical central bore. The radiograph was generated at 290 kV, 16 mA-min, FFD 2.5 m with film D4, see Fig. 5. The reconstructed profile shows constant values of g in the ranges of the propellant and the hollow interior.

It should be noted that asymmetry in the product caused by local density variation, e.g., by voids, results in a concentric ring of lower g value in the reconstructed profile. In many applications, the presence of such a ring can be used as a rejection criterion of the product.

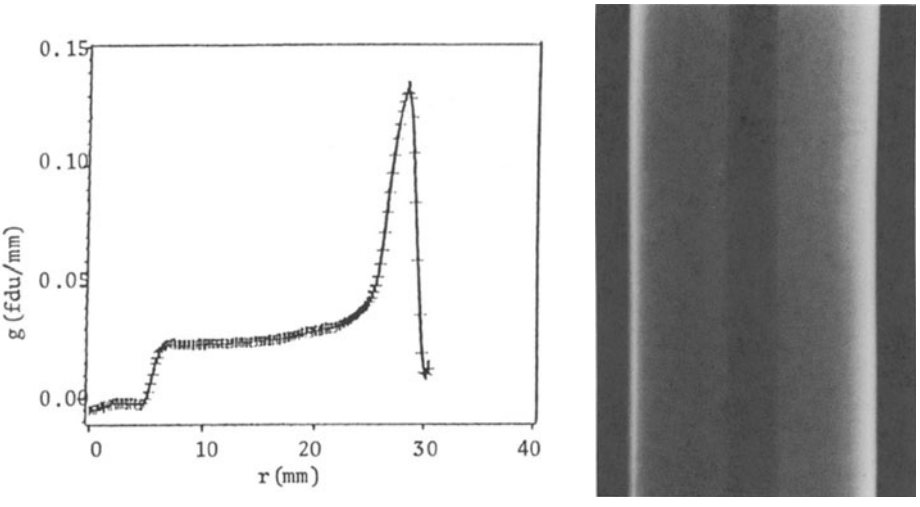


Fig. 5 Radiograph of a propellant charge with a cylindrical bore and metallic case (6 cm radius, 290 kV) - right. Reconstructed profile - left.

## CONCLUSIONS

Tomography from a single projection is a useful low-cost method for NDT classification of products. The algorithms mentioned present a workable solution of the inverse problem suitable for real-time systems. This single-projection tomography is also a useful simple tool for the study of the beam-hardening phenomena and additional distortions (PSF, scattering edge effects, etc.) as the results are more transparent than with the CT systems.

## ACKNOWLEDGEMENT

D. Pal received a post-doctoral fellowship from the Pikovsky-Valazzi fund.

REFERENCES


1. R. Rangayyan, A.P. Dhawa and R. Gordon, "Algorithm for Limited-View CT", Applied Optics, Vol. 24 (1985), p. 4000.
2. K.C. Tam, J.W. Eberhard and K.W. Mitchell, "Limited-Angle X-ray CT Image Reconstructions in Industrial NDT" in J. Boogaard and G.M. Van Dijk, Proc. of the 12th World Conf. on NDT, Elsevier Science Pub. (Amsterdam, 1989), Vol. 1, p. 766.
3. K.C. Tam and L.J. Thomas III, "Digital Tomography Incorporating A Priori Information", present QNDE Conf.
4. M.L.H. Siao and J.W. Eberhard, "A Model-Based Reconstruction Method for Incomplete Projection Industrial CT Imaging", present QNDE Conf.
5. A. Notea, D. Pal and M. Deutsch, "Density Distribution in Cylindrically Symmetric Objects From a Single Radiographic Image", in J. Farley and R.W. Nichols, NDT, Proc. 4-th Euro. Conf., Vol. 3, p. 2093, Pergamon Press (1988).
6. D. Pal, A. Notea, M. Deutsch, "Single Projection Tomography of Objects With Cylindrical Symmetric Density Distribution", Trans. Isr. Nucl. Soc., Vol. 14 (1987), p. VI-31.
7. M. Deutsch, A. Notea and D. Pal, "Reconstruction of Discontinuous Density Profiles of Cylindrical Symmetric Objects From Single X-ray Projections", Applied Optics, Vol. 27 (1988), p. 3962.
8. M. Deutsch, A. Notea and D. Pal, "Abel Reconstruction of Piecewise Constant Radial Density Profiles From X-ray Radiographs", Applied Optics 28 (1989), p. 3183.
9. M. Deutsch and J. Beniamini, "Derivative-Free Inversion of Abel's Integral Equation", Appl. Phys. Lett., Vol. 41 (1982), p. 27.
10. M. Deutsch and I. Beniamini, "Inversion of Abel's Integral Equation for Experimental Data", J. Appl. Phys., Vol. 54 (1983), p. 137.